Star Formation Newsletter #354 57-64

武藤恭之

Wavelike nature of the vertical shear instability in global protoplanetary disks

Eleonora Svanberg, Can Cui, Henrik N. Latter ★

The vertical shear instability (VSI) is a robust phenomenon in irradiated protoplanetary disks (PPDs). The majority of previous numerical simulations have focused on the turbulent properties of its saturated state. However, the saturation of the VSI manifests as large-scale coherent radially travelling inertial waves. In this paper, we study inertial-wave-disk interactions and their impact on VSI saturation. Inertial-wave linear theory is developed and applied to a representative global 2D simulation using the Athena++ code. It is found that the VSI saturates by separating the disk into several radial wave zones roughly demarcated by corotation resonances (turning points); this structure also manifests in modest radial variations in the vertical turbulence strength. Future numerical work should employ large radial domains to accommodate this radial structure of the VSI, while concurrently adopting sufficiently fine resolutions to resolve the parametric instability that attacks the saturated VSI inertial waves.

- 原始惑星系円盤における、Vertical Shear Instability の線形解析と非線形数値計算
- z 方向に構造がある場合に生じる、z 方向の過安定モード
  - 高さ方向には、一般に密度変化などがある
- z 方向を考慮した局所線形解析で、分散関係・位相速度・群速度などを計算
  - 動径方向の波の振る舞いに注目、位相速度と群速度は逆向き
  - 動径方向の、ある限られた範囲でしか波が存在しない
- グローバルな、軸対称 2 次元計算で、線形解析の結果と飽和状態を確認
  - n=1 のモードが卓越
  - やった計算の結果では、円盤が動径方向に 4 つの領域に分かれた

局所線形解析の基礎方程式

$$\frac{\partial \rho}{\partial t} + \mathbf{u}\cdot\nabla\rho = -\rho\nabla\cdot\mathbf{u},$$
$$\frac{\partial \mathbf{u}}{\partial t} + \mathbf{u}\cdot\nabla\mathbf{u} = -\frac{1}{\rho}\nabla P - 2\Omega\boldsymbol{e}_z\times\mathbf{u} - \nabla\Phi,$$

背景流

$$\mathbf{u}_0 = -\frac{3}{2}\Omega x\boldsymbol{e}_y,$$
$$\rho_0 = \rho_{\rm mid}\,\exp[-z^2/(2H^2)]$$

摂動　$\tilde{\rho} = \rho'(z)\mathrm{e}^{\mathrm{i}k_x x - \mathrm{i}\omega t}$　など：軸対称

z 方向の摂動方程式

$$\frac{d^2h'}{dz^2} - \frac{z}{H^2}\frac{dh'}{dz} + \frac{\xi}{H^2}h' = 0$$
$$\xi = \frac{\omega^2}{\Omega^2} - H^2k_x^2\left(\frac{\omega^2}{\omega^2-\Omega^2}\right)$$

分散関係式、n は z 方向のモード

$$\omega^4 - \left[\Omega^2(n+1) + c_s^2k^2\right]\omega^2 + \Omega^4 n = 0$$

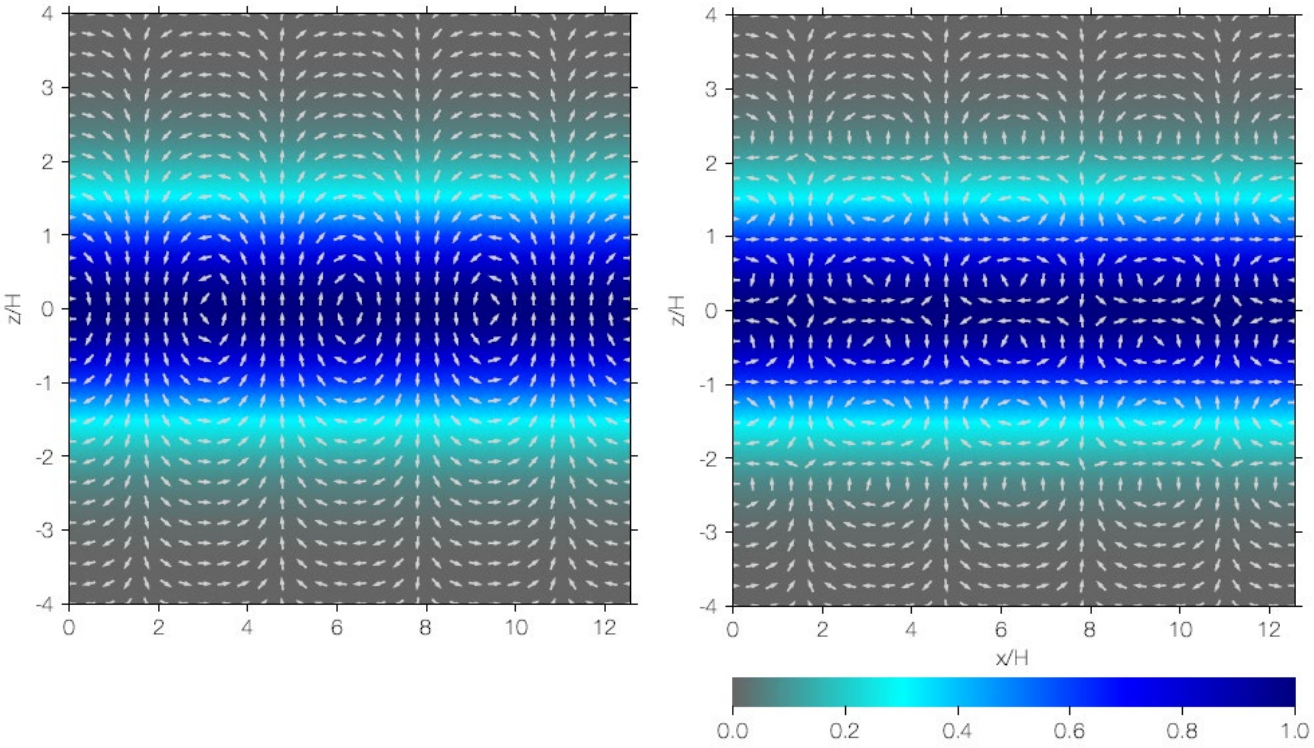

n=1 と n=6 の固有関数（色は背景の密度）

動径方向の波数：ゼロになる場所が波の反射位置

$$c_s^2 k_x^2 = \frac{(\Omega^2 - \omega^2)(n\Omega^2 - \omega^2)}{\omega^2}$$

群速度：符号は位相速度と逆向きになる

$$c_{\rm g} = \frac{d\omega}{dk_x} = \mp \frac{c_s}{1 + \Omega^2/\omega^2}$$

数値計算：軸対称・グローバル、Newtonian Cooling 入り

コード： Athena++

$$\frac{\partial \rho}{\partial t} + \nabla \cdot (\rho \mathbf{v}) = 0,$$
$$\frac{\partial (\rho \mathbf{v})}{\partial t} + \nabla \cdot (\rho \mathbf{v}\mathbf{v} + P\mathbf{I}) = -\rho \nabla \Phi,$$
$$\frac{\partial E}{\partial t} + \nabla \cdot (E + P)\mathbf{v} = -\rho(\mathbf{v} \cdot \nabla \Phi) - \Lambda_{\rm c}$$

平衡状態：

$$\rho(R, z) = \rho_0 (R/R_0)^{-q_{\rm D}} \exp\left[\frac{GM}{c_s^2}\left(\frac{1}{r} - \frac{1}{R}\right)\right],$$
$$\Omega(R, z) = \Omega_{\rm K}[-(q_{\rm D} + q_{\rm T})h^2 + (1 - q_{\rm T}) + q_{\rm T} R/r]^{1/2}.$$

500周期後のスナップショット

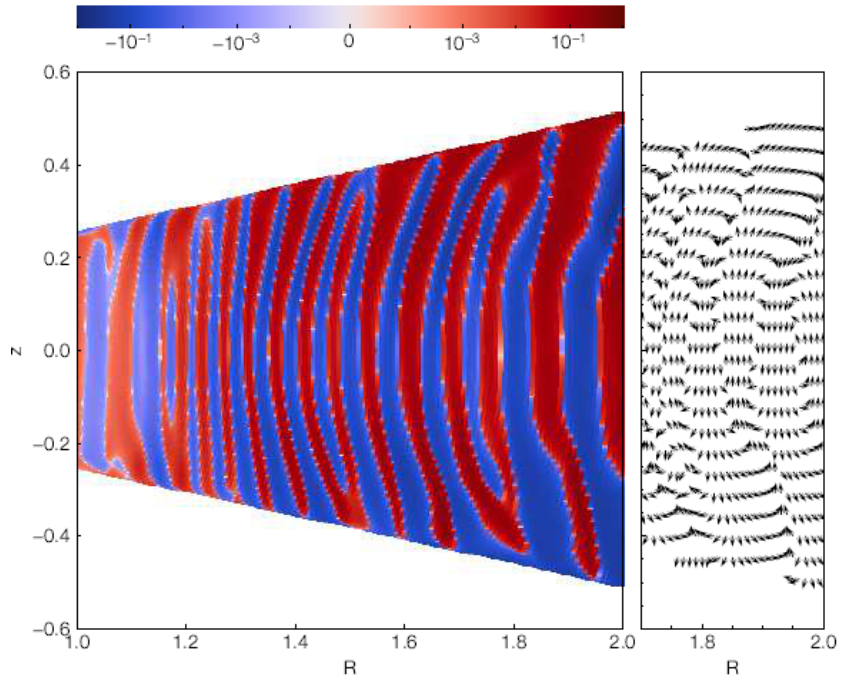

動径方向の波数：ゼロになる場所が波の反射位置

$$c_s^2 k_x^2 = \frac{(\Omega^2 - \omega^2)(n\Omega^2 - \omega^2)}{\omega^2}$$

群速度：符号は位相速度と逆向きになる

$$c_{\rm g} = \frac{d\omega}{dk_x} = \mp \frac{c_s}{1 + \Omega^2/\omega^2}$$

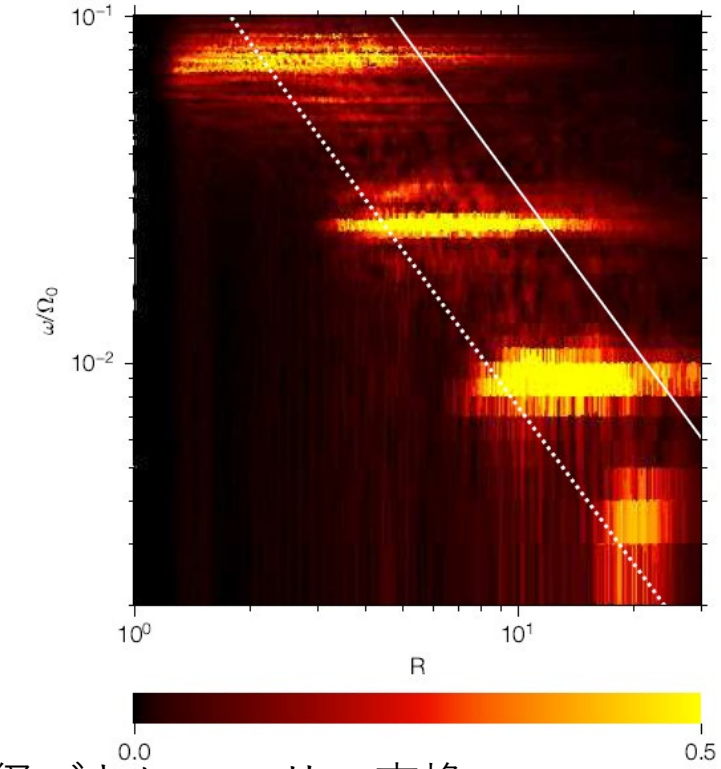

半径ごとにフーリエ変換
４種類の波が、それぞれの領域に出ている

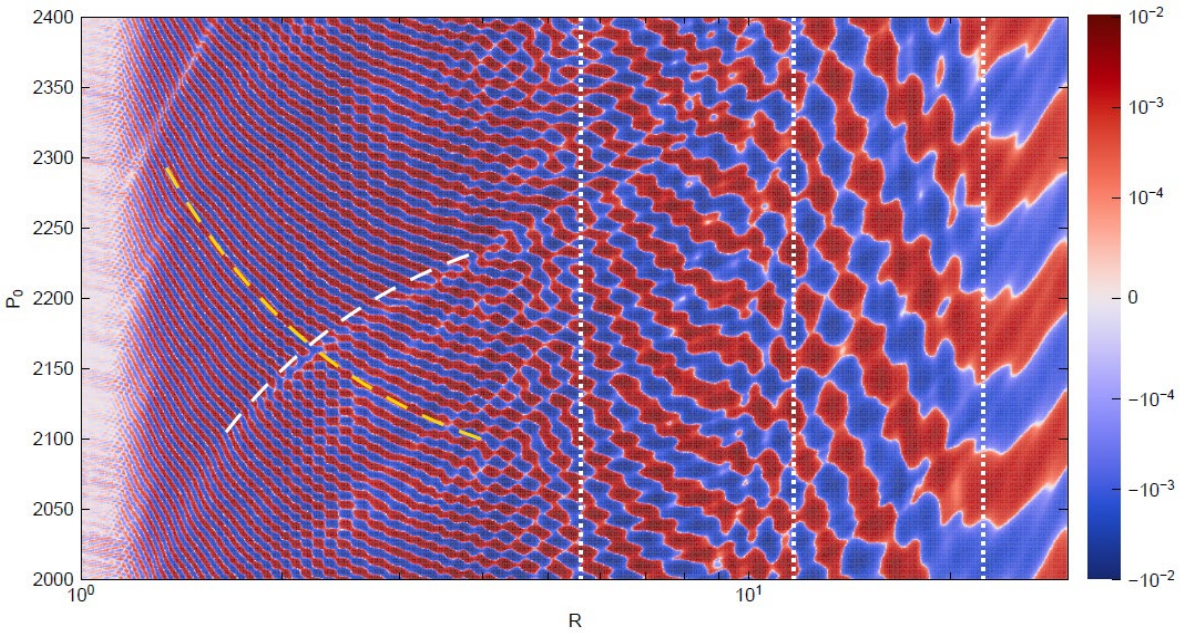

中心面速度の時間変化：
- ４つの領域に分かれている
- 黄色線が位相速度、白線が群速度。線形解析の結果を描いているが、数値計算とよく一致

No. 59

How cooling influences circumbinary discs

Prakruti Sudarshan, Anna B. T. Penzlin, Alexandros Ziampras, Wilhelm Kley, Richard P. Nelson ★
Circumbinary disc observations and simulations show large, eccentric inner cavities. Recent work has shown that the shape and size of these cavities depend on the aspect ratio and viscosity of the disc, as well as the binary eccentricity and mass ratio. It has been further shown that, for gaps created by planets, the cooling timescale significantly affects the shape and size of the gap. In this study, we consider the effect of different cooling models on the cavity shape in a circumbinary disc. We compare locally isothermal and radiatively cooled disc models to ones with a parametrised cooling timescale (β-cooling), implemented in 2D numerical simulations for varying binary eccentricities. While the shape of the cavity for radiative and locally isothermal models remains comparable, the inner disc structure changes slightly, leading to a change in the precession rate of the disc. With β-cooled models, the shape and size of the cavity changes dramatically towards values of β=1. Based on our findings, we introduce a parametrised β model that accounts for the shorter cooling timescale inside the cavity while adequately reproducing the results of the radiative model, and we highlight that accurate treatment of the thermodynamics inside the cavity has a significant impact in modelling circumbinary systems.

- 周連星円盤に生じる中心付近の穴の形状が、cooling prescription によってどのように変わるかを、数値シミュレーションで調べる
- 局所等温・β-cooling・放射冷却の場合を調べる
- 局所等温の計算と、放射冷却の計算は、穴の形状がほぼ同じだが、穴の歳差運動の速さが少し異なる
- β-cooling の場合は、穴の形状は大きく異なり、β=1 のあたりで最も穴が小さくなる。冷却時間が長くても、放射冷却の場合とあまり一致しない
  - 局所的な温度・密度の情報を使って、冷却時間を変えるようにすると、一致は良くなる

基礎方程式：

$$\frac{\partial \Sigma}{\partial t} + \nabla \cdot (\Sigma \boldsymbol{u}) = 0,$$
$$\frac{\partial \Sigma \boldsymbol{u}}{\partial t} + \nabla \cdot \left(\Sigma \boldsymbol{u} \otimes \boldsymbol{u} + P\mathbf{I} - \overline{\mathbf{\Pi}} \right) = \Sigma \boldsymbol{g},$$
$$\frac{\partial e}{\partial t} + \nabla \cdot \left((e + P - \overline{\mathbf{\Pi}})\boldsymbol{u} \right) = \Sigma \boldsymbol{u} \cdot \boldsymbol{g} + Q.$$

温度の扱いとして３通り：

(1) 局所等温：円盤の温度分布を決め打ち　$T = \dfrac{\mu \mathrm{G} M_{\mathrm{co}}}{\mathcal{R}} \dfrac{h^2}{r}.$　冷却がよく効く場合に対応

(2) ベータ冷却：ある温度分布になるように冷却時間をパラメータで設定

$$\frac{\partial T}{\partial t} = -\frac{T - T_0}{\beta} \Omega_{\mathrm{K}} = \frac{Q_{\mathrm{relax}}}{\Sigma c_{\mathrm{v}}}$$

(3) 放射冷却：その場の光学的厚みに応じて放射冷却、冷却が効きにくい場合に対応

$$\frac{\partial \Sigma c_{\mathrm{v}} T}{\partial t} = -2\sigma_{\mathrm{SB}} \frac{T^4}{\tau_{\mathrm{eff}}} = Q_{\mathrm{cool}} \qquad \tau_{\mathrm{eff}} = \frac{3}{8}\tau + \frac{\sqrt{3}}{4} + \frac{1}{4\tau + \tau_{\mathrm{min}}}$$

数値計算の設定：

・局所等温、ベータの値が 0.01, 1, 100 の場合、放射冷却の場合を調べる
・バイナリーの離心率が 0, 0.15, 0.3, 0.5 の場合について、それぞれ調べる
・二次元計算、Pluto コード、(Nr, Nphi)=(684, 1168)
・周連星系円盤にできた穴の長半径と離心率がどう変わっていくかを調べる

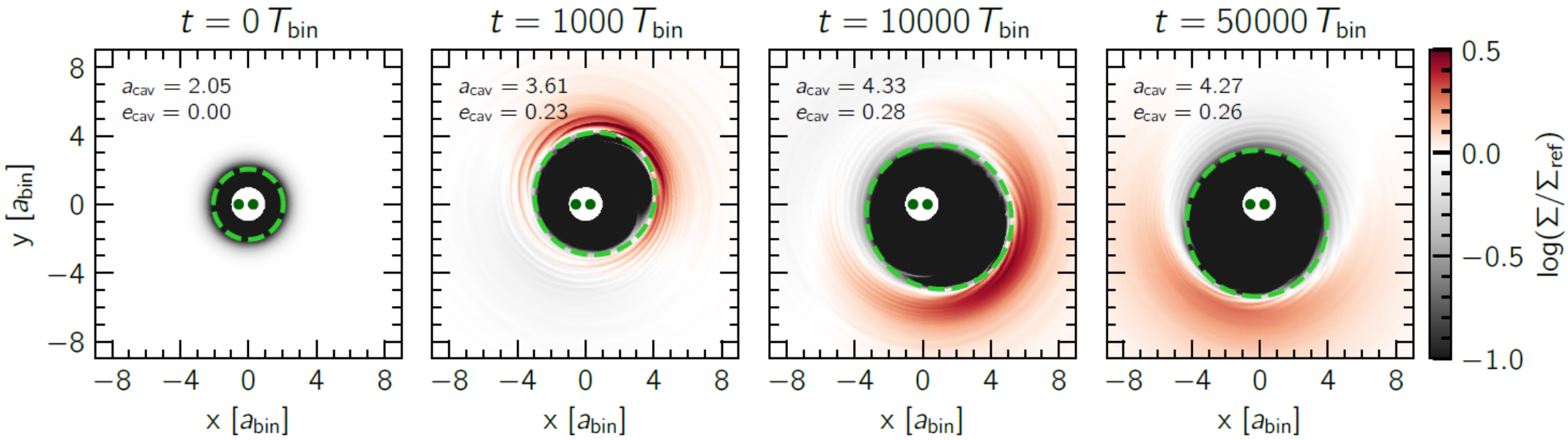

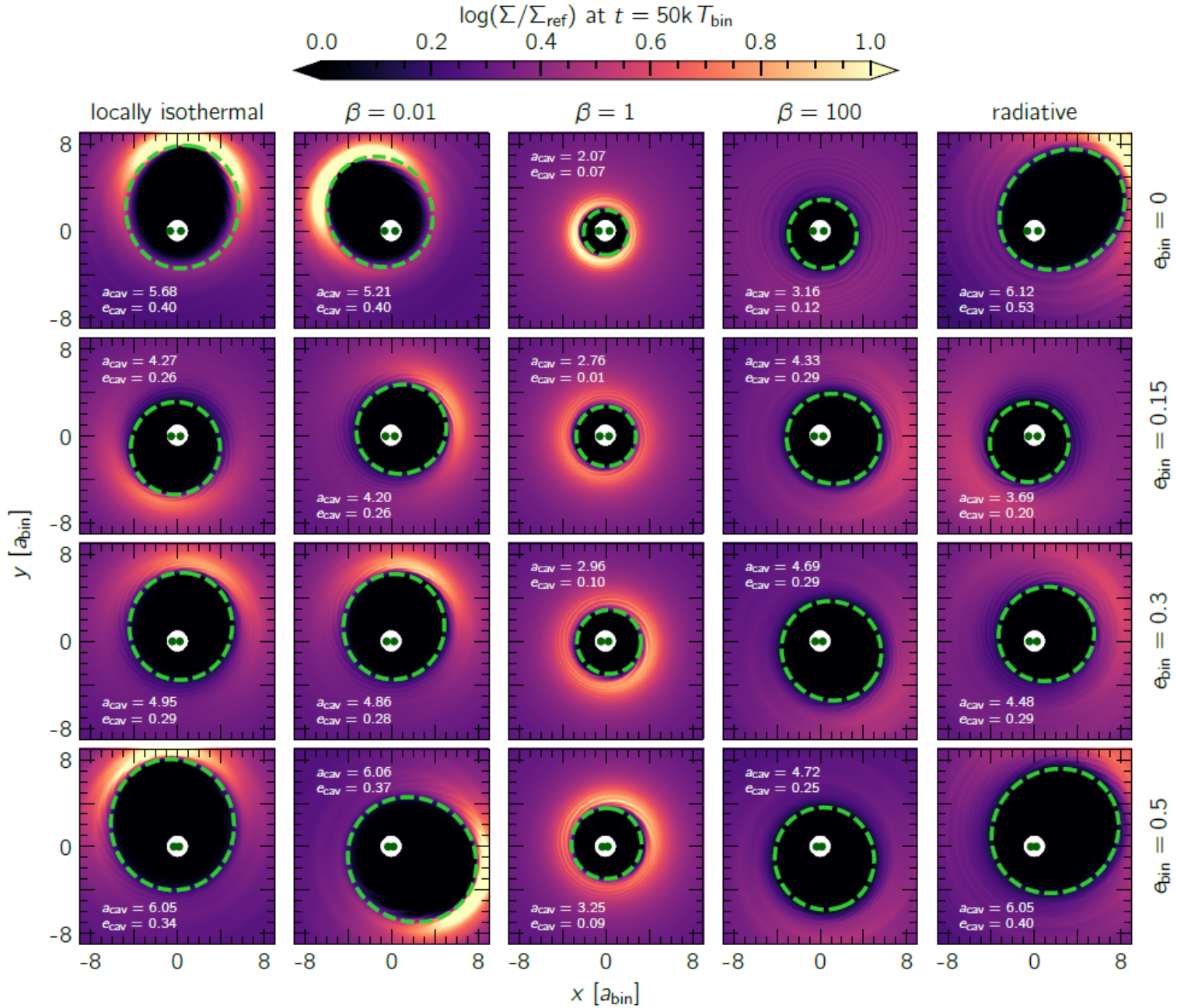

バイナリー周期で 5万周後の様子

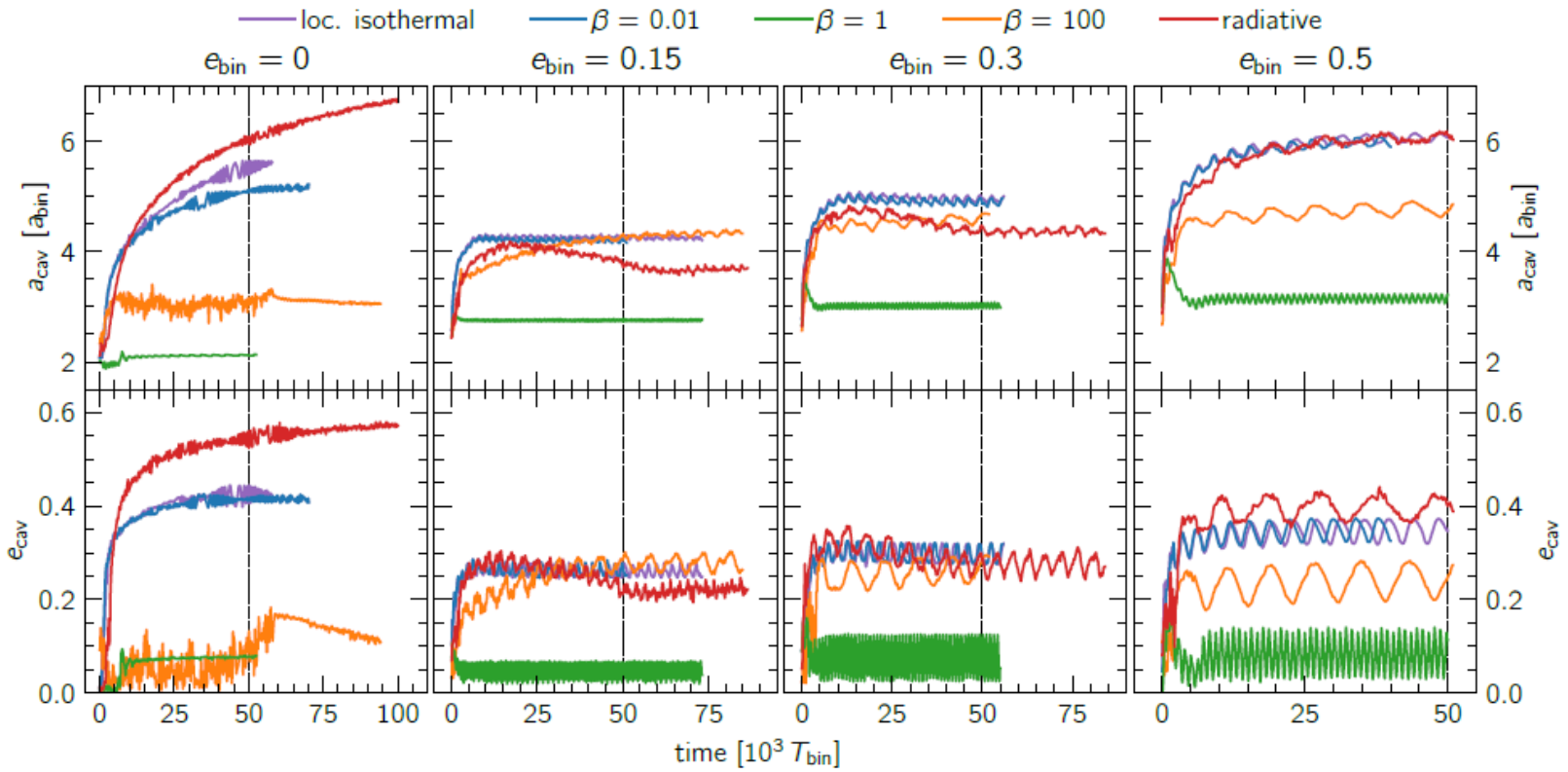

穴の長半径と離心率の進化

- 局所等温と輻射冷却のモデルは同じような様子
  - 穴の部分は非常に薄いので、冷却が利き、局所等温と似たような振る舞いになる
- 冷却時間を大きくしても、輻射冷却のモデルに一致しない
  - 冷却時間が密度に依らないので、密度の薄い内側で冷却が効かず、温度が高く、圧力が大きい状態になる。このため、内側円盤をより押し込み、穴が小さくなる
  - 冷却時間とケプラー時間が同程度のモデルが、穴が最も小さくなっている

ベータ冷却で、輻射冷却に似たような結果を得る方法

密度が小さい場所では、ベータを下げて冷却時間を短くする

$$\log\beta(\Sigma) = \log\beta_{\rm ref} - (2 + \log\beta_{\rm ref}) \cdot \frac{\Sigma_{\rm th} - \Sigma}{\Sigma_{\rm th}}, \quad \Sigma \le \Sigma_{\rm th},$$

その場の温度・密度に応じて、適したベータの値を与える

$$\frac{\partial e}{\partial t} \sim \frac{e}{t_{\rm cool}} = |Q_{\rm cool}| \Rightarrow \beta = \frac{\Sigma c_{\rm v} T}{|Q_{\rm cool}|}\Omega_{\rm K}$$

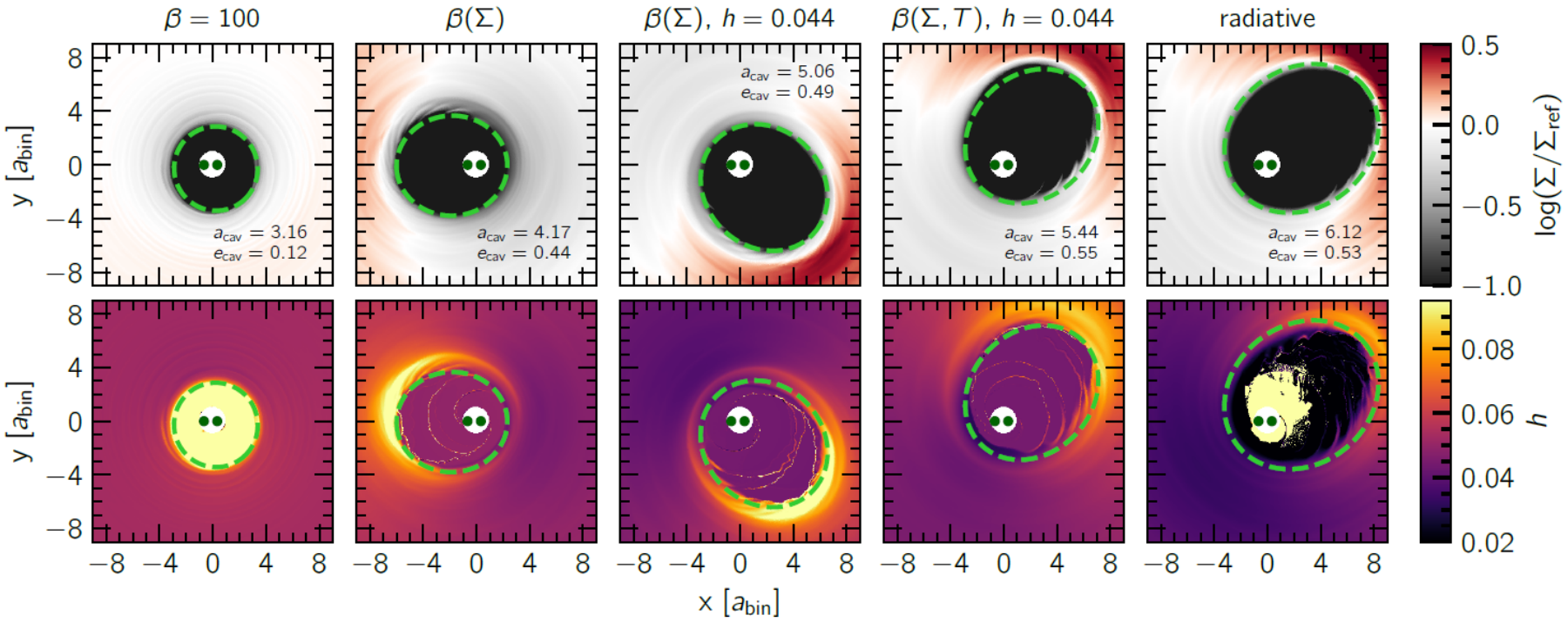

No. 62

The Musca molecular cloud: The perfect "filament" is still a sheet

A. Tritsis, F. Bouzelou, R. Skalidis, K. Tassis, T. Enßlin, G. Edenhofer ★ The true 3-dimensional (3D) morphology of the Musca molecular cloud is a topic that has received significant attention lately. Given that Musca does not exhibit intense star-formation activity, unveiling its shape has the potential of also revealing crucial information regarding the physics that dictates the formation of the first generation of stars within molecular clouds. Here, we revisit the shape of Musca and we present a comprehensive array of evidence pointing towards a shape that is extended along the line-of-sight dimension: (a) 3D maps of differential extinction; (b) new non-local thermodynamic equilibrium radiative transfer simulations of CO rotational transitions from a sheet-like, magnetically-dominated simulated cloud; (c) an effective/critical density analysis of available CO observations; (d) indirect consequences that a filamentary structure would have had, from a theoretical star-formation perspective. We conclude that the full collection of observational evidence strongly suggests that Musca has a sheet-like geometry.

- Musca 分子雲の三次元構造の推定。観測的には、フィラメント状に見える
- 奥行構造がどうなっているかを、観測をもとに議論
  - Gaia, 2MASS, Pan-STARRS, ALL-WISE の観測から、三次元構造を再構成した結果、奥行きは数 pc 程度ある
  - シート形状の分子雲の MHD シミュレーションをもとに、 12CO2-1, 3-2, 4-3 のラインを計算した結果、観測とよく似たライン形状になった
- Musca は、奥行き方向に広がったシート形状をしているものと推定

異なる波長の extinction による奥行きの推定：色々な視線で、奥行きを推定する
※多波長の観測から奥行きを推定するコードを、著者たちが開発している

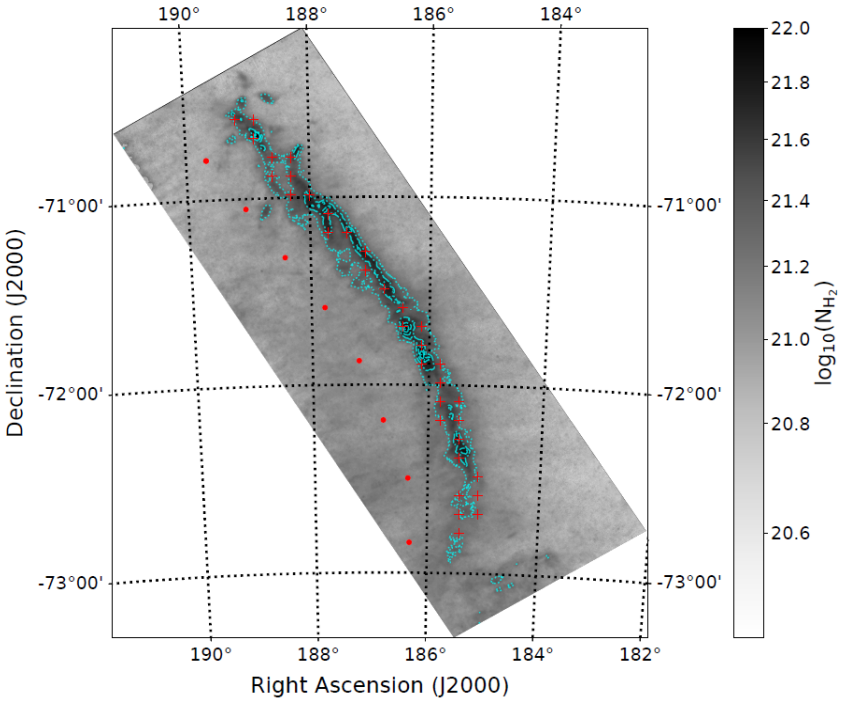

Musca 分子雲の様子

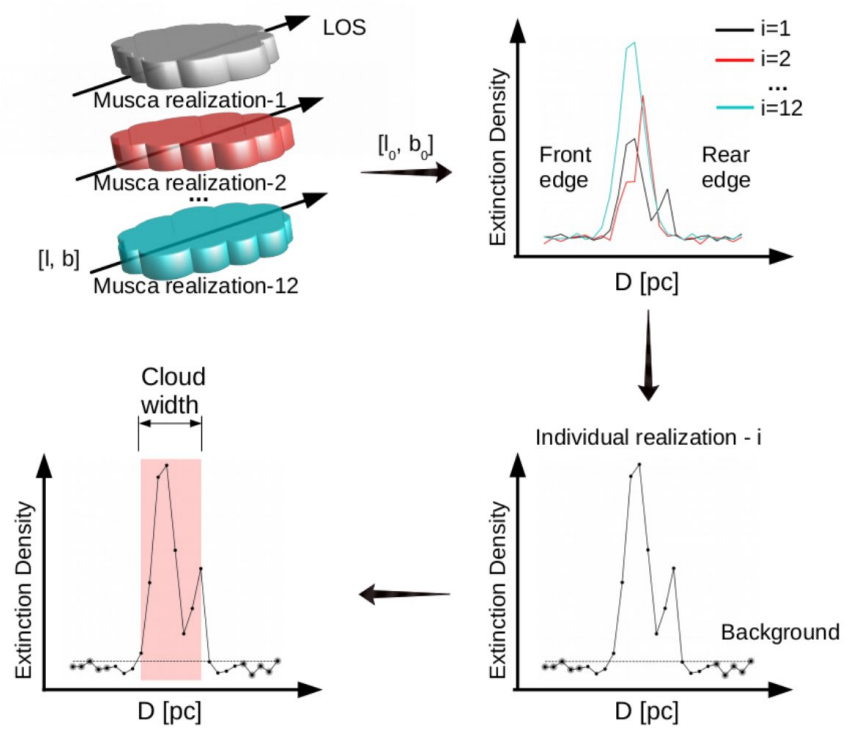

手法
- 一つの視線につき、同じような extinction を出すいくつかのモデルをもとに、三次元構造を再構築

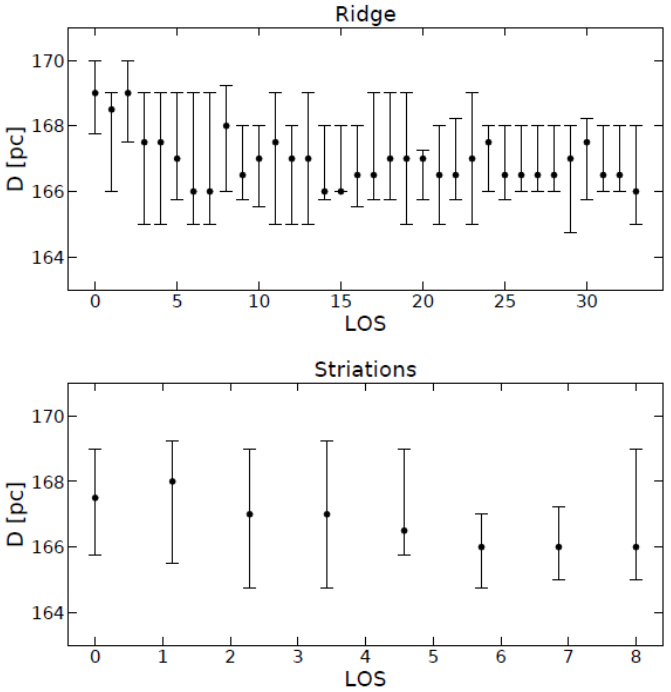

結果
- どの視線でも、およそ 6pc 程度の奥行きがある

シート状分子雲のMHDシミュレーションをもとにした、12CO 輝線のモデルと観測

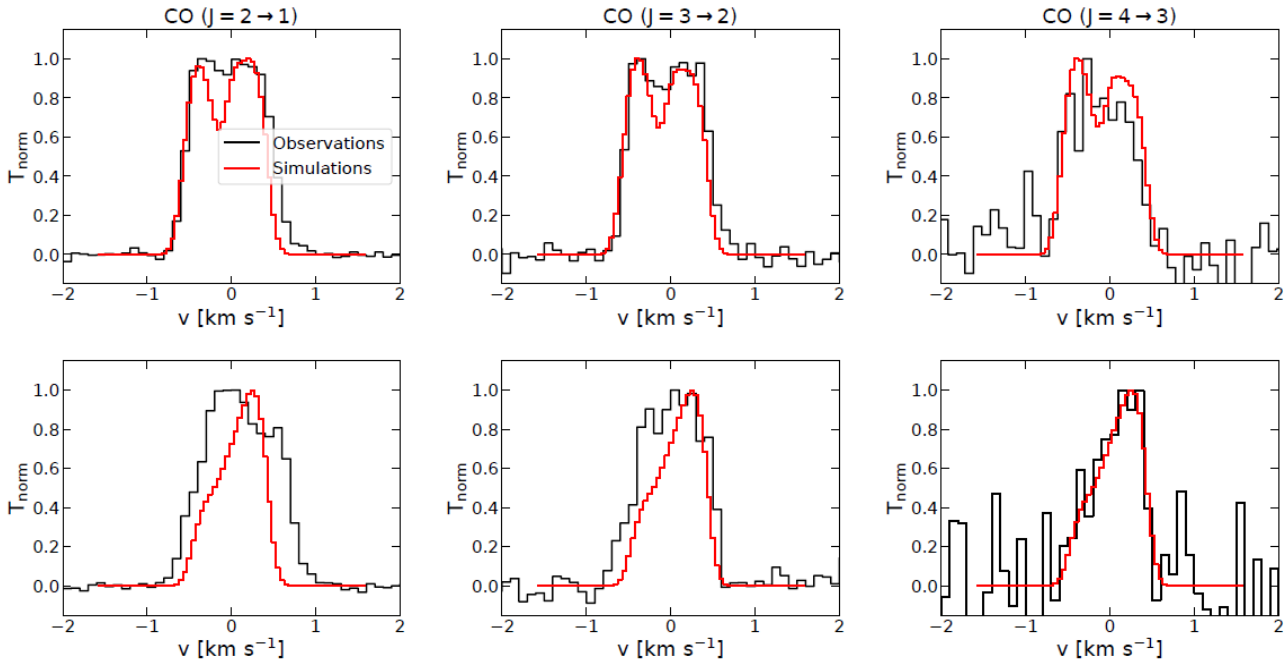

Musca の北（上パネル）と南（下パネル）
のライン形状をどちらも再現できる

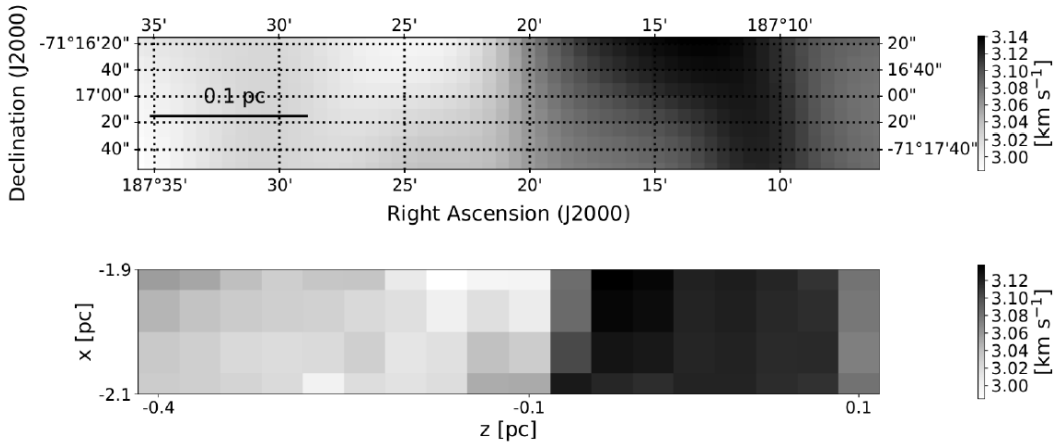

Musca のモーメント 1 マップの比較
上が観測、下がモデル

No. 58

Pulsational instability of pre-main-sequence models from accreting protostars II. Modelling echelle diagrams of δ Scuti stars without rotational splitting

T. Steindl, K. Zwintz, M. Müllner ★
The physics of early stellar evolution (e.g. accretion processes) is often not properly included in the calculations of pre-main-sequence models, leading to insufficient model grids and hence systematic errors in the results. We aim to investigate current and improved approaches for the asteroseismic modelling of pre-main-sequence delta Scuti stars. We calculated an extensive grid of pre-main-sequence models including the early accretion phase and used the resulting equilibrium models as input to calculate theoretical frequency spectra. These spectra were used to investigate different approaches in modelling echelle diagrams to find the most reliable methods. By applying Petersen diagrams, we present a simple algorithm to extract echelle diagrams from observed pulsation frequencies. We show that model grids with insufficient input physics and imperfect modelling approaches lead to underestimated uncertainties and systematic errors in the extracted stellar parameters. Our re-discussion of HD 139614 leads to different stellar parameters than the ones derived by Murphy et al. (2021). We performed a model comparison between this previous investigation and our results by applying the Akaike and Bayesian information criteria. While the results with regard to our 10-d model are inconclusive, they show (very) strong evidence of a 6-d model with fixed accretion parameters (leading to almost identical stellar parameters to those of the 10-d model) to be preferred over the model applied by Murphy et al. (2021). In general, our modelling approach can provide narrow constraints on the stellar parameters (Δ R $\sim$ 0.05 $R_\odot$, Δ log g $<$ 0.01, and Δ $M_\star$ 0.1 $M_\odot$). The extensively tested modelling approaches and automatic extraction of echelle diagrams should allow us to study many more pre-main-sequence delta Scuti stars in the future and lead to reliable stellar parameters.

No. 60

Nonradial and nonpolytropic astrophysical outflows. XI. Simulations of the circumstellar environment of RY Tau

C. Sauty, R. M. G. de Albuquerque, V. Cayatte, J. J. G. Lima, J. F. Gameiro

★ Context. There are recent observational evidences that RY Tau may present two different outflow stages, a quiescent one and a more active one. We try to model that phenomenon. Aims. We have performed new 2.5D magneto-hydrodynamical simulations of the possible accretion-outflow environment of RY Tau based on analytical solutions to reduce the relaxation time. Methods. We used as initial conditions the analytical self-similar solution we used to model the RY Tau micro jet. In the closed field line region of the magnetosphere we have reversed the direction of the flow and increased the accretion rate by increasing the density and the velocity. We have also implemented the heating rate and adjusted it according to the velocity of the flow. The accretion disk is treated as a boundary condition. Results. The simulations show that the stellar jet and the accreting magnetosphere attain a steady state in only a few stellar rotations, confirming the robustness and stability of self-similar solutions. Additionally, two types of behavior were observed similar to the one observed in RY Tau. Either the steady stellar outflow and magnetospheric inflow are separated by a low static force free region or the interaction between the stellar jet and the magnetospheric accretion creates coronal episodic mass ejections originating from the disk and bouncing back onto the star. Conclusions. The ratio of mass loss rate to mass accretion rate that coincides with the change of behaviour observed in RY Tau, lays within the range of ratios that have been measured during the period of the micro jet initial analysis.

No. 61

A graph theory-based multi-scale analysis of hierarchical cascade in molecular clouds : Application to the NGC 2264 region

B. Thomasson, I. Joncour, E. Moraux, C. Crespelle, F. Motte, Y. Pouteau, T. Nony

★ The spatial properties of small star-clusters suggest that they may originate from a fragmentation cascade of the cloud for which there might be traces up to a few dozen of kAU. Our goal is to investigate the multi-scale spatial structure of gas clumps, to probe the existence of a hierarchical cascade and to evaluate its possible link with star production in terms of multiplicity. From the Herschel emission maps of NGC 2264, clumps are extracted using getsf software at each of their associated spatial resolution, respectively [8.4, 13.5, 18.2, 24.9, 36.3]". Using the spatial distribution of these clumps and the class 0/I Young Stellar Object (YSO) from Spitzer data, we develop a graph-theoretic analysis to represent the multi-scale structure of the cloud as a connected network. From this network, we derive three classes of multi-scale structure in NGC 2264 depending on the number of nodes produced at the deepest level: hierarchical, linear and isolated. The structure class is strongly correlated with the column density N_{H_2} since the hierarchical ones dominate the regions whose $N_{H_2} > 6 \times 10^{22} cm^{-2}$. Although the latter are in minority, they contain half of the class 0/I YSOs proving that they are highly efficient in producing stars. We define a novel statistical metric, the fractality coefficient F that measure the fractal index describing the scale-free process of the cascade. For NGC 2264, we estimate F = 1.45±0.12. However, a single fractal index fails to fully describe a scale-free process since the hierarchical cascade starts at a 13 kAU characteristic spatial scale. Our novel methodology allows us to correlate YSOs with their multi-scale gaseous environment. This hierarchical cascade that drives efficient star formation is suspected to be both hierarchical and rooted by the larger-scale gas environment up to 13 kAU.

No. 63

Hot methanol in the [BHB2007] 11 protobinary system: hot corino versus shock origin? : FAUST V

C. Vastel et al. - FAUST team

★ Methanol is a ubiquitous species commonly found in the molecular interstellar medium. It is also a crucial seed species for the building-up of the chemical complexity in star forming regions. Thus, understanding how its abundance evolves during the star formation process and whether it enriches the emerging planetary system is of paramount importance. We used new data from the ALMA Large Program FAUST (Fifty AU STudy of the chemistry in the disk/envelope system of Solar-like protostars) to study the methanol line emission towards the [BHB2007] 11 protobinary system (sources A and B), where a complex structure of filaments connecting the two sources with a larger circumbinary disk has been previously detected. Twelve methanol lines have been detected with upper energies in the range [45-537] K along with one 13CH3OH transition. The methanol emission is compact and encompasses both protostars, separated by only 28 au and presents three velocity components, not spatially resolved by our observations, associated with three different spatial regions, with two of them close to 11B and the third one associated with 11A. A non-LTE radiative transfer analysis of the methanol lines concludes that the gas is hot and dense and highly enriched in methanol with an abundance as high as 1e-5. Using previous continuum data, we show that dust opacity can potentially completely absorb the methanol line emission from the two binary objects. Although we cannot firmly exclude other possibilities, we suggest that the detected hot methanol is resulting from the shocked gas from the incoming filaments streaming towards [BHB2007] 11 A and B, respectively. Higher spatial resolution observations are necessary to confirm this hypothesis.

No. 64

The growth and migration of massive planets under the influence of external photoevaporation

Andrew J. Winter, Thomas J. Haworth, Gavin A. L. Coleman, Sergei Nayakshin ★
The formation of gas giant planets must occur during the first few Myr of a star's lifetime, when the protoplanetary disc still contains sufficient gas to be accreted onto the planetary core. The majority of protoplanetary discs are exposed to strong ultraviolet irradiation from nearby massive stars, which drives winds and depletes the mass budget for planet formation. It remains unclear to what degree external photoevaporation affects the formation of massive planets. In this work, we present a simple one dimensional model for the growth and migration of a massive planet under the influence of external FUV fields. We find that even moderate FUV fluxes $F_{\rm FUV} \gtrsim 100\,G_0$ have a strong influence on planet mass and migration. By decreasing the local surface density and shutting off accretion onto the planet, external irradiation suppresses planet masses and halts migration early. The distribution of typical stellar birth environments can therefore produce an anti-correlation between semi-major axis and planet mass, which may explain the apparent decrease in planet occurrence rates at orbital periods $P_{\rm orb} \gtrsim 10^3$ days. Even moderate fluxes $F_{\rm FUV}$ strongly suppress giant planet formation and inward migration for any initial semi-major axis if the stellar host mass $M_* \lesssim 0.5\,M_\odot$, consistent with findings that massive planet occurrence is much lower around such stars. The outcomes of our prescription for external disc depletion show significant differences to the current approximation adopted in state-of-the-art population synthesis models, motivating future careful treatment of this important process.